Finite Element Analysis and Test of Damping Torque of Eddy Current Damper for Docking Mechanism

LUO Ling, YANG Fei-fei, WANG Yan-fang, LIU Jing-lin
(School of Automation, Northwestern Polytechnical University, Xi'an 710072, China)

Abstract: An eddy current damper is considered to be most suitable for energy absorption of the docking system in space, its damping torque is the most important for energy absorption, but there is no general method to solve the damping torque analytically. An eddy current damper used for docking mechanism is presented in this paper, which is very similar to a coreless permanent magnet generator. The influences of parameters of the eddy current damper on the damping torque at the given volume are discussed. The structure, the simulation models and the test system scheme of the eddy current damper are introduced firstly, and effects of number of magnetic poles, as well as conductivity, length, thickness and mean diameter of the rotor on the damping torque are analyzed, finite element analysis and test are employed to perform the analysis. Finally, an equation to express the relationship between the damping torque and these parameters is presented. The discrepancies between torque values obtained by the equation and experimental test for a few prototypes are reasonable, thus showing that the damping torque equation could help to proceed with the design of an eddy current damper for docking mechanism.

Key words: Eddy currents damper; Docking mechanism; Finite element method; Testing; Damping Torque
CLC number: TM351 **Document code**: A **Article ID**: 1000-1328(2011)05-1026-09
DOI: 10.3873/j.issn.1000-1328.2011.05.010

对接机构的涡流阻尼器阻尼力矩的有限元仿真和试验分析

罗 玲, 杨菲菲, 王燕芳, 刘景林
(西北工业大学自动化学院, 西安 710072)

摘 要: 涡流阻尼器可以很好吸收航天器交会对接时产生的碰撞能量,其阻尼力矩直接关系其对碰撞能量的吸收,但没有通用的阻尼力矩计算公式。通过对研发的对接机构用涡流阻尼器样机的有限元仿真和实验,分析其阻尼力矩。介绍了对接机构的涡流阻尼器样机的结构、2D 和 3D 电磁场有限元仿真模型和阻尼力矩测试系统,分析了涡流阻尼器的磁极对数、转子材料导电率、转子长度、转子厚度、转子平均直径对阻尼力矩的影响,给出了阻尼力矩的计算公式。计算结果表明,对铝合金转子涡流阻尼器样机,阻尼力矩的计算值与实测值误差小,对铜合金转子涡流阻尼器样机,阻尼力矩的计算值与实测值误差较大。分析结果有助于对接机构用涡流阻尼器的研制。

关键词: 涡流阻尼器; 对接机构; 有限元法; 测试; 阻尼力矩

0 Introduction

The docking system is one of the most important functions for the space station and the orbiter such as space shuttle[1-2]. The development of the docking system needs variably controlled actuators for energy absorption, compliance control and adjustment of a docking interface to eliminate misalignments[1,3]. An eddy

收稿日期:2010-03-14; 修回日期:2010-12-11

current damper is considered to be most suitable for energy absorption of the docking system in space[4-5]. An eddy current damper can remove energy from the system without ever contacting the structure, which allows for maintenance and lubrication free operation, its applications include structure vibration suppression[6], speed reduction or braking system in vehicle[7-8], vibration control of rotary machinery[9], and vibration isolation enhancement in levitation systems[10].

For different applications, there are different configurations of eddy current damper. The eddy current damper used for docking mechanism in this paper is very similar to a coreless permanent magnet generator. Since the eddy current problem usually depends on the geometry of the moving conductor and the pole shape, there is no general method for solving its braking torque analytically.

In this paper, the study is focus on the relationship between the braking torque and the parameters of the eddy current damper. The structure, the simulation models and the test system scheme of the damper are introduced first, followed by analysis on the relationship of the torque with the magnetic poles number, the influences on braking torque of conductivity, length, thickness and mean diameter of the conductor are analyzed, finite element simulation and test are employed to perform the analysis. The FEA software is Infolytica's MagNet 2D and 3D. All the analysis is done for the same volume of the eddy current dampers. Finally, an equation to express the relationship between the braking torque and the parameters is presented. The comparison between the torque values obtained by the equation and test for a few prototypes is made.

1　Configuration, analysis model and test system

1.1　Configuration

The eddy current damper consists of two main sections: stator and rotor. Different from the stator in [11], this stator includes permanent magnets and two parts made of ferromagnetic material, which are inner stator and outer stator. A few pieces of permanent magnet are mounted and bound on the surface of the inner stator. The rotor includes the conductor and the shaft. The conductor is placed in the air gap between the outer stator and the permanent magnets, and it is a hollow cylinder rather than the metallic rigid core in [11]. Fig. 1 depicts the eddy current damper configuration. While the shaft is rotated by other mechanism drive, the conductor rotates in the air gap magnetic field generated by the permanent magnets, and eddy currents form in the conductor. Interaction between induced eddy currents and permanent magnet magnetic field produces a force and braking torque, which retards the rotation of the mechanism and dissipates the energy supplied by the mechanism.

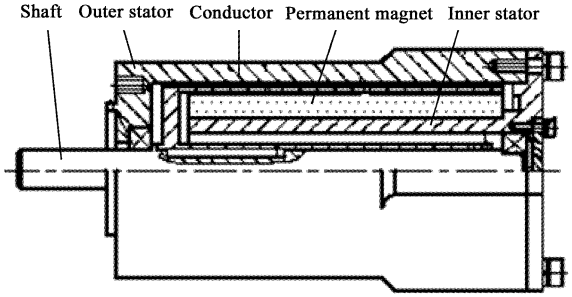

Fig. 1　Configuration of the eddy current damper

1.2　Analysis model

Fig. 2(a) and 2(b) give the 2D and 3D finite element analysis model, respectively. Both models are built by MagNet software. The 2D model shows the cross section configuration of the eddy current damper, it can not indicate the end section of the eddy current damper, so the contributions to the braking torque of the conductor bottom and the end magnetic field are ignored in the 2D simulation, which increases the discrepancy between the 2D simulation value and the test value of the braking torque for the prototype. And when the relationship of the braking torque and the conductor length is studied, in order to save the fabricating cost of prototypes and shorten the fabricate time, the conductor length is changed and the other parts lengths are kept constant. The 2D model cannot reflect the length difference between the conductor and the other parts of the prototypes, which the 3D model can

do. Therefore the 3D model simulates the prototype more accurate than the 2D model, but the simulation time of 3D model is much longer than the one of 2D model. The discrepancies between the 2D simulation value and the test value of the braking torque for the prototypes of different conductor lengths are more than those for the prototypes of different conductor materials, thicknesses and mean diameters and different pole numbers. So the 3D model is employed just for studying the influence on the braking torque of the conductor length.

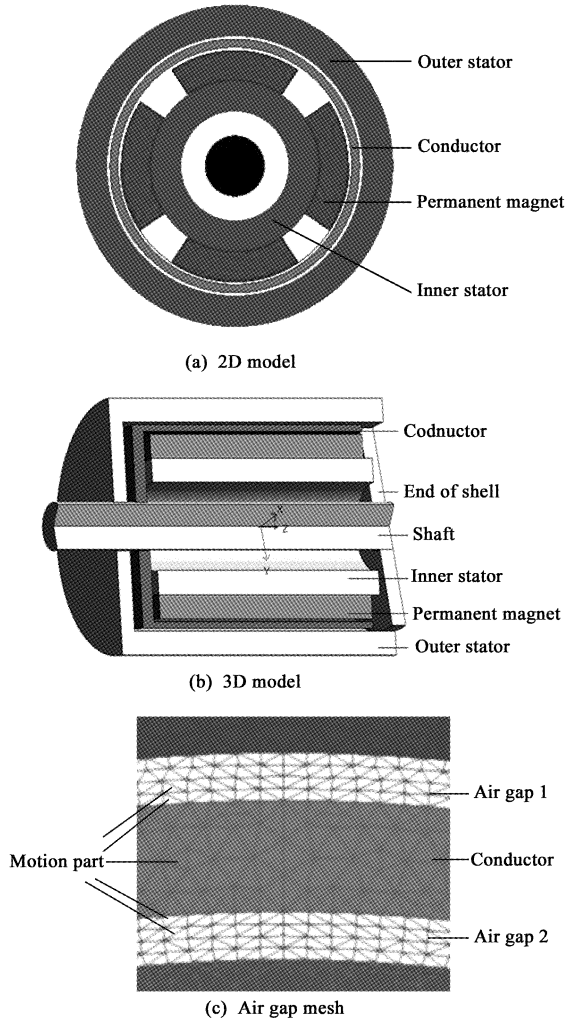

Fig. 2 Finite element analysis model

To reduce the mesh time and improve the analysis accuracy, two air gaps, air gap 1 being between the outer stator and the conductor, air gap 2 between the conductor and the permanent magnets, are divided into four layers respectively as shown in Fig. 2(c). Two layers next to the conductor of air gap 1 and those of air gap 2 are set as the motion. The conductor is set as the motion too. The solvers employed to calculate the torque-speed curves of the eddy current damper are 2D Transient with Motion and 3D Transient with Motion (constant speed) in 2D FEA and 3D FEA, respectively.

1.3 Test system

Fig. 3 gives the block diagram of prototype test. The eddy current damper is driven by a synchronous motor instead of the real docking mechanism. A converter is employed to set the speed of the synchronous motor to 500r/min, 1000 r/min, 2000r/min to 5000 r/min with the speed interval of 500 r/min. For every set speed, a torque-meter is used to measure the braking torque of the eddy current damper as soon as the speed-meter shows that the synchronous motor drives the eddy current damper to the set speed. In order to reduce the influence of the conductor temperature rise in the eddy current damper on the braking torque, the torque measure should be done as quickly as possible. After the torque is measured, the synchronous motor should be stop first, when the thermometer shows that the conductor temperature has fallen to the ambient temperature, the next test should be started.

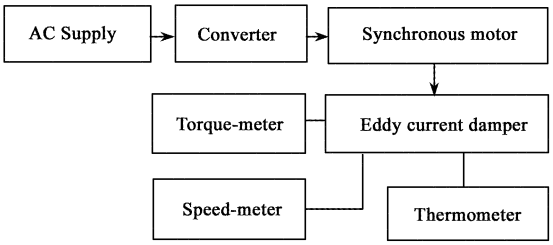

Fig. 3 Block diagram of prototype test

2 Pole numbers

The prototype of 2 poles and another one of 4 poles have been made. Torque-speed curves of prototypes are simulated by 2D FEA and tested, all of the curves are shown in Fig. 4, and the torque-speed curve of an eddy current damper model with 6 poles is calculated by 2D FEA, the curve is also shown in Fig. 4. The difference of all the prototypes and models is only the pole numbers. The material, length, mean diame-

ter and thickness of the conductor are aluminum alloy, 0.0495m, 0.0245m and 0.0008m respectively.

Fig. 4 shows that the calculated torque is larger than the measured one at the same speed. This discrepancy is due to the conductivity of the conductor varies with the temperature. When the speed is slow, since the energy dissipated is small, the conductor's temperature almost keeps constant in process of test. When the speed is fast, the conductor's temperature goes up quickly, which results in decreases of both the induced eddy currents and the torque. However, the conductivity of the conductor keeps constant during the 2D simulation. This is why the discrepancy between the calculated torque and the measured one at the faster speed is larger than the discrepancy between them at the slower speed.

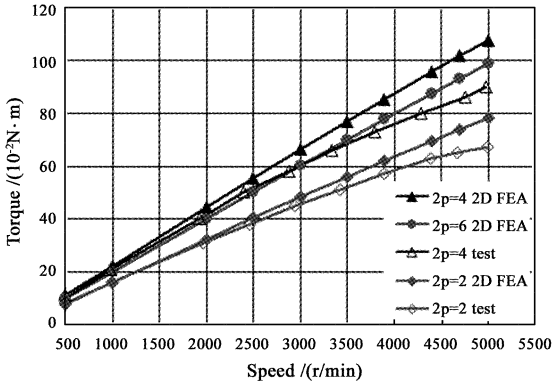

Fig. 4　Torque-speed curves at different pole numbers

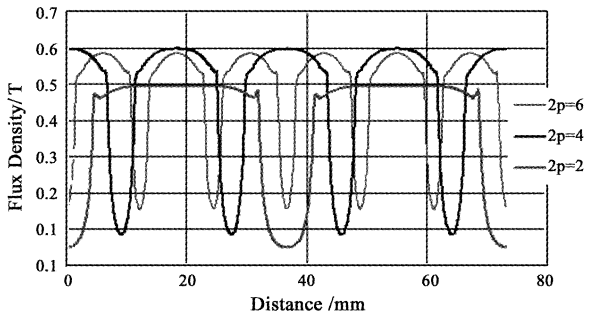

Fig. 5　Air gap flux density at different pole numbers

Compare the torque values obtained with 2D FEA of eddy current dampers for different pole numbers, it is found that the torque of 4 poles eddy current damper is the greatest, and the one of 2 poles eddy current damper is the smallest. Fig. 5 shows that the peak value of air gap flux density of 4 poles is the greatest, and the one of 2 poles is the smallest. But table 1 shows the average air gap flux density of 6 poles is the largest. The air gap flux density waveforms shape of different pole numbers are not the same, which means there are different harmonics components. The harmonic analysis results of the air gap flux density waveforms are given in table 2, which show the fundamental frequency component value of the air gap flux density of 4 poles is the largest, the one of 2 poles is the smallest. Therefore the torque value at different pole numbers is related with the fundamental frequency component value of the air gap flux density.

Table 1　Average air gap flux density Bav of different pole numbers 2p

2p	2	4	6
Bav /T	0.3968	0.4779	0.4848

Table 2　Harmonic values of air gap flux density

Harmonic order	2p = 2	2p = 4	2p = 6
1	0.57530	0.68944	0.66868
2	0	0.00034	0.00017
3	0.06477	0.08707	0.07911
4	0	0.00026	0.00018
5	0.05591	0.03564	0.03031
6	0	0.00010	0.00017
7	0.07873	0.06170	0.05537

3　Conductivity

The larger the conductivity is, the greater the eddy currents and the braking torque are. The electrical conductivity of the material is simply defined as isotropic and constant in 2D FEA. For the prototypes, the poles number is 4, and the length, mean diameter and thickness of the conductor are 0.0495m, 0.0245m and 0.0008m respectively. While conductor materials are copper alloy and aluminum alloy, the torque-speed curves of test and 2D FEA are illustrated in Fig. 6. It shows the torque of copper alloy conductor is larger than the one of aluminum alloy conductor at the same speed. Table 3 gives the electrical conductivity σ of copper alloy and aluminum alloy. There are also dis-

crepancies between the test curves and the calculation one. For the copper alloy conductor, the calculation torque is less than the test one, while for the aluminum alloy conductor it is larger than the test one. This is likely due to the error between the ideal conductivity and the real conductivity of the material.

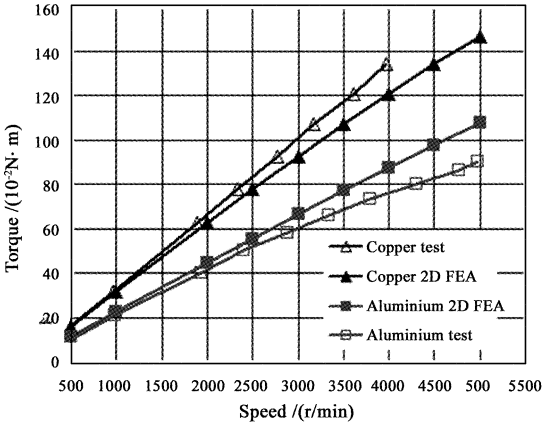

Fig. 6 Torque-speed curves for different conductor material

Table 3 Conductivity σ of conductor material

Material	Copper alloy	Aluminum alloy
σ (10^7 S/m)	3.248	1.734

4 Conductor length

The induced voltage of the conductor increases linearly with the conductor length, so the eddy currents and the braking torque are proportional to the conductor length. To save the fabricating cost of prototypes, only three prototypes are made, which conductor's length is 0.0495 m, 0.04 m and 0.018 m respectively, but all of them shared the same 4 poles stator. And the material, mean diameter and thickness of the conductor are aluminum alloy, 0.0245m and 0.0008m respectively. In 2D model of MagNet, the length in axis direction of all the parts for the eddy current damper are assumed as the same, so the 3D model shown in Fig. 2 (b) is also employed to calculate the torque-speed curve.

Fig. 7 shows the torque-speed curves of prototypes with different conductor length. Fig. 8 gives the torque-conductor length curves while the speed is 3500r/min. It can be found that the discrepancy be-

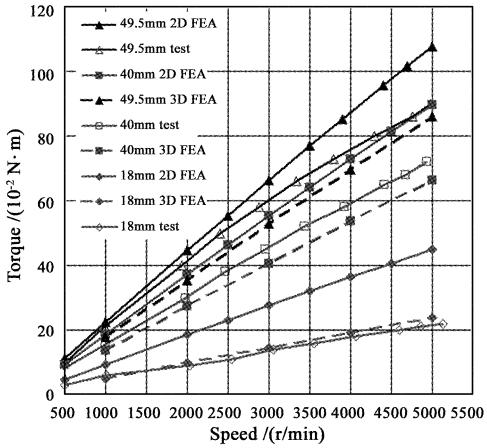

Fig. 7 Torque-speed curves for different conductor length

tween the calculated torque by 3D FEA and the test torque is less than the one between the calculated torque by 2D FEA and the test torque. And all of the curves indicate that the braking torque is proportional to the conductor length.

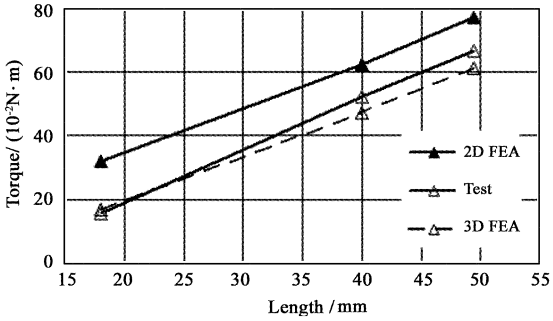

Fig. 8 Torque-conductor length curve at 3500r/min

5 Conductor thickness

Sharifaddin and Kourosh[11] proposed that in the presence of a time varying magnetic field the current density in conductor varies exponentially inward from the surface. The distance h in which the current density decreases to 1/e of its surface value is called the nominal depth of penetration that is given by the relation

$$h = \sqrt{\frac{2\rho}{\omega\mu}} \tag{1}$$

Where ρ is the resistivity of the conductor in ohm-meter, and μ is the absolute permeability of the conductor.

For the aluminum alloy conductor, ρ is $5.767 \times 10^{-8}\Omega$m, μ is 12.567×10^{-7}H/m, according to equation(1), h is 13.24mm while ω is 523.599 rad/s

(5000r/min). As for the prototypes studied in this paper, the conductor thickness is less than 1mm, so the influence of skin effect on braking torque can be ignored.

To analyze the influence of the conductor thickness on braking torque, the thickness of the conductor is changed by changing its inner and outer diameters and keeping its mean diameter and the sizes of both stators and the permanent magnets constant. Therefore when the thickness of the conductor is enlarged, the air gap length is shortened. For the prototypes studied here, the poles number is 4, and the material, length and mean diameter of the conductor are aluminum alloy, 0.0495m, and 0.0245m respectively.

Fig. 9 gives the torque-conductor thickness curve calculated by 2D FEA while speed is 3500r/min. It clearly indicates the greater the conductor thickness is, the greater the torque is.

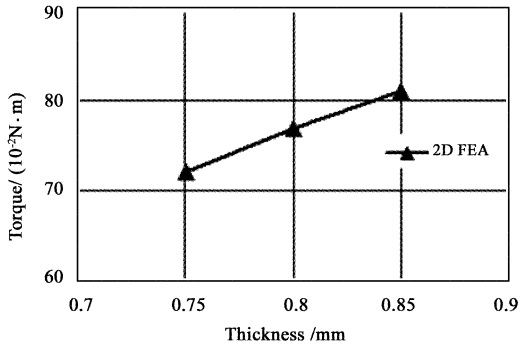

Fig. 9　Torque-conductor thickness curve at 3500r/min

6　Conductor mean diameter

The conductor mean diameter D_{cm} is defined as equation (2).

$$D_{cm} = \frac{D_{co} + D_{ci}}{2} \qquad (2)$$

Where D_{co} is the outer diameter of the conductor, and D_{ci} is the inner diameter of the conductor.

There are two ways to change the conductor mean diameter, one changing its inner and outer diameter and keep the sizes of permanent magnets and outer stator constant, another changing its inner and outer diameter and the size of permanent magnets and outer stator. The common of the two ways is to keep the conductor thickness constant. The difference is that the air gap length is varied for the former, while it is constant for the latter. For the prototypes studied here, the poles number is 4, and the material, and length of the conductor are aluminum alloy and 0.0495m respectively.

A. The air gap length is varied

When the conductor inner diameter and outer diameter are enlarged with the same value to enlarge the mean diameter, the thickness of the conductor, the sizes of the outer stator and permanent magnet are kept constant, therefore, the length of air gap 1 became shorter, while the length of air gap 2 became longer, which is shown in Fig. 10(b).

Line 1 in Fig. 12 is the torque-conductor mean diameter curve obtained with 2D FEA at speed of 3500r/min.

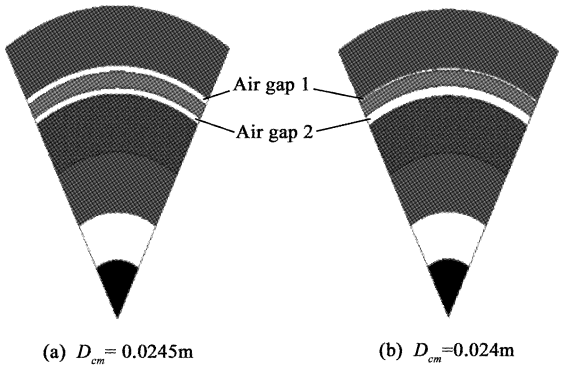

Fig. 10　Part of the 2D model with different mean diameter and air gap length

B. The air gap length is constant

As the conductor inner diameter and outer diameter are enlarged with the same value, at the same time the inner diameter of the outer stator and the outer diameter of permanent magnet are enlarged, then the length of both air gaps and the length in radial direction of permanent magnet are kept constant, which means the length in radial direction of the outer stator is shortened and the length in radial direction of the inner stator is enlarged, which is shown in Fig. 11(b).

Line 2 in Fig. 12 is the torque-conductor mean diameter curve obtained with 2D FEA at speed of 3500r/min.

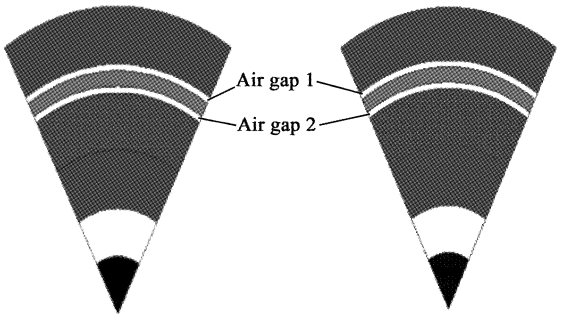

Fig. 11 Part of the 2D model with different mean diameter and same air gap length

Fig. 12 shows that the bigger the conductor mean diameter is, the larger the braking torque is. And the increase magnitude of the braking torque with the conductor mean diameter for the varied air gap length is far less than the one for the constant air gap length.

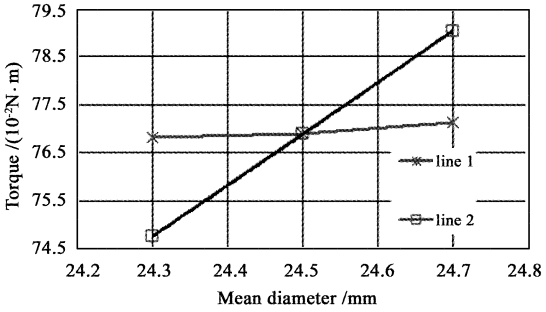

Fig. 12 Torque-conductor mean diameter curve at 3500r/min

7 Braking torque equation

Sharifaddin and Kourosh[11] introduced that eddy current brakes employ complicated mathematical relations in operation caused by factors like skin effect, nonlinearity of property of magnetic materials, unpredictability in path of induced current, end effect and thermal effects and variation in conductivity due to temperature variation. Therefore, they presented the torque equation (3) for an ideal situation.

$$T = \frac{\pi}{4}\frac{1}{\rho}B_0^2 R^4 L\omega \qquad (3)$$

At the equation (3) ω is angular speed of the rotor, B_0 is magnetic intensity of the stator in air gap at zero speed, L is rotor length, R is radius of the rotor and ρ is resistivity of the rotor.

According to equation (3) and based on the analysis presented above, the torque of our eddy current damper for an ideal situation should be calculated by equation (4).

$$T = \frac{\pi}{4}\frac{1}{\rho}B_0^2 L\omega\left[\left(\frac{D_{cm}+h_c}{2}\right)^4 - \left(\frac{D_{cm}-h_c}{2}\right)^4\right]$$
$$= \frac{\pi}{4}\sigma B_0^2 L\omega\left[\left(\frac{D_{cm}+h_c}{2}\right)^4 - \left(\frac{D_{cm}-h_c}{2}\right)^4\right] \qquad (4)$$

At the equation (4) h_c is the rotor thickness. The physical properties of the prototypes are listed in Table 4.

Table 4 Physical properties of the prototypes

Property	Value			
	No. 1	No. 2	No. 3	No. 4
σ /(10^7S/m)	3.248	3.248	1.734	1.734
B_0 /T	0.5753	0.6894	0.5753	0.6894
L /m	0.0495	0.04	0.0495	0.04
D_{cm} /m	0.0245	0.0245	0.0245	0.0245
h_c /m	0.0008	0.0008	0.0008	0.0008

The conductors of prototype 1 and prototype 2 are made of copper alloy, while those of prototype 3 and prototype 4 are made of aluminum alloy. The conductor length and the pole numbers of prototype 1 and prototype 3 are the same, 0.0495m of length and 2 poles respectively, while those of the rest are the same, 0.04m of length and 4 poles respectively. Fig. 13 shows the torque values obtained with equation (4) and tested.

Fig. 13 indicates that the torque calculated is greater than the test one for the prototypes of copper alloy conductor and for the prototype of aluminum alloy conductor with 4 poles stator when the speed is faster than 3000r/min, while the torque calculated is less than the test one for the prototype of aluminum alloy conductor with 2 poles stator, and for the prototype of aluminum alloy conductor with 4 poles stator when the speed is slower than 3000r/min.

8 Conclusions

At the given volume of the eddy current damper, the comparisons between the torque-speed curves of the eddy current damper with different pole numbers indicate that the pole numbers' influence on the torque is decided by the fundamental frequency component value

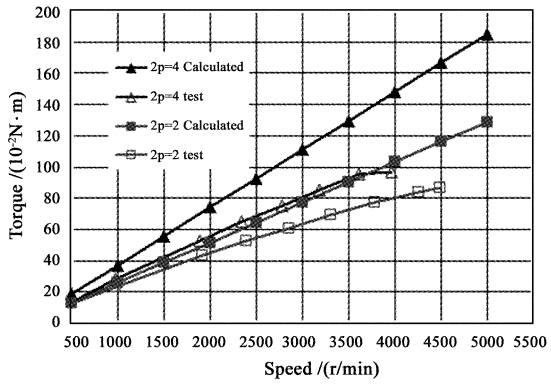

(a)　Copper alloy conductor

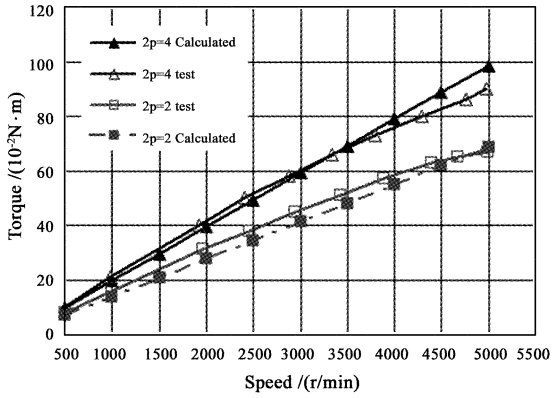

(b)　Aluminum alloy conductor

Fig. 13　Torque-speed curves calculated and tested

of the air gap flux density rather than the pole numbers itself. The analysis of the torque-speed curves for the eddy current damper with different conductor material, length, thickness and mean diameter indicate that the braking torque is proportional to the conductivity of the conductor material and the conductor length, and the greater the thickness and mean diameter of the conductor are, the greater braking torque of the eddy current damper is. The relationships of braking torque and the parameters can be expressed as equation (4) for an ideal situation. Of all the conductor geometry parameters shown in equation (4), the contribution to the braking torque of the mean diameter is much more than the one of the length. In order to reach a higher air gap flux density, the thickness of the conductor is very small compared to the length and diameter, its value is less than 1 millimeter generally, so its influence on the braking torque is also the smallest. Equation (4) and the values of each physical property show that the contribution to the braking torque of the air gap flux density is much more than those of the conductor geometry parameters, and the influence on the braking torque of the conductivity is the most important. However, the weight of the eddy current damper used for the docking mechanism should be reduced to the minimum for the given braking torque, so the conductor material should be selected not only by the conductivity and also by the densities.

Although equation (4) does not take account of the armature reaction, end effect, nonlinearity of property of magnetic materials, etc, the discrepancy between the torque obtained with equation (4) and the one tested for the prototypes show it is helpful to proceed with the design of an eddy current damper for docking mechanism.

References

[1] Niwa S, Suzuki M, Kimura K. An electric shock absorbing system for the docking mechanisms in space[C]. The 17th International Symposium on Space Technology and Science, Tokyo, Japan, May 20 - 25, 1990.

[2] Tian H, Zhao Y, Zhang D W. Movement simulator modeling and simulation in integrate test platform for docking mechanism[J]. Journal of Astronautics, 2007,28(4):233 - 238(in Chinese).

[3] Yang F, Qu G J. Analysis of mechanismic transmission principle for the diffrentialy mechanical-electronical buffer damping system in a spacial butt mechanism[J]. Mechanics and Practice Journal, 2000,22(6):51 - 54(in Chinese).

[4] Lou H W, Qu G J, Liu J S. Spacial butt mechanism[M]. Beijing:Aviation Industry Press,1992:128 - 130(in Chinese).

[5] Zhao Y, Cao X B, Xu Y R. Study on parameter optimization of electromagnetic brake in space docking mechanisms[J]. Space Science Journal, 2000, 20(4):366 - 372(in Chinese).

[6] Henry A S, Sze K C. Novel eddy current damping mechanism for passive magnetic bearings [C]. 48th AIAA/ASME/ ASCE/ AHS/ASC, Structures, Structural Dynamics and Materials Conference, Honolulu, USA, April 23 - 26, 2007.

[7] Gay S E, Ehsani M. Parametric analysis of eddy-current brake performance by 3-D finite-element analysis[J]. IEEE Trans. Magn., 2006,42(2):319 - 328.

[8] Zhao X B, Ji C Y. Analysis of flux leakage in novel permanent magnet type eddy current retarder for vehicle applications[C].

Vehicle Power and Propulsion Conference, Harbin, China, September 3 – 5, 2008.

[9] Fung R F, Sun J H, Su S M. Vibration control of the rotating flexible-shaft/multi-flexible-disk system with the eddy current damper[J]. ASME Journal of Vibration and Acoustics, 2002, 124(4): 519 – 526.

[10] Zheng J, Deng Z G, Zhang Y, et al. Performance improvement of high temperature superconducting maglev system by eddy current damper[J]. IEEE Trans. Appl. Supercond., 2009, 19(3): 2148 – 2151.

[11] Sharifaddin Sharif and Kourosh Sharif. Influence of skin effect on torque of cylindrical eddy current brake[C]. International Conference on Power Engineering, Energy and Electrical Drives, Lisbon, Portugal, March18 – 20, 2009.

Luo Ling(1970 –), received her Ph.D in 2004, Professor. Her main research focus on the theory and design of rare earth permanent magnet electrical machine.

Address: P. O. Box 352 of Northwestern Polytechnical University (710072)

Tel: (029)88431336

E-mail: luoling@nwpu.edu.cn

(编辑:曹亚君)